HYDROACOUSTIC SIGNATURES OF COLORADO RIVERBED SEDIMENTS IN MARBLE AND GRAND CANYONS USING MULTIBEAM SONAR

Daniel Buscombe, Research Geologist, US Geological Survey, Southwest Biological Science Center, Grand Canyon Monitoring and Research Center, Flagstaff, AZ, dbuscombe@usgs.gov;
Paul E. Grams, Research Hydrologist, US Geological Survey, Southwest Biological Science Center, Grand Canyon Monitoring and Research Center, Flagstaff, AZ, pgrams@usgs.gov;
Matt A. Kaplinski, Research Associate, School of Earth and Environmental Sustainability, Northern Arizona University, Flagstaff, AZ, matt.kaplinski@nau.edu;
Robert Tusso, Hydrologist, US Geological Survey, Southwest Biological Science Center, Grand Canyon Monitoring and Research Center, Flagstaff, AZ, rtusso@usgs.gov;
David M. Rubin, Research Professor, Department of Earth and Planetary Sciences, University of California Santa Cruz, Santa Cruz, CA, drubin@ucsc.edu

INTRODUCTION

Characterizing the large-scale sedimentary make-up of heterogeneous riverbeds (Nelson et al., 2014), which consist of a patchwork of sediment types over small scales (less than one to several tens of meters) (Dietrich and Smith, 1984) requires high resolution measurements of sediment grain size. Capturing such variability with conventional physical (e.g. grabs, cores, and dredges) or underwater photographic sampling (Rubin et al., 2007; Buscombe et al., 2014a) would be prohibitively costly and time-consuming. However, characterizing bed sediments using high-frequency (several hundred kilohertz) acoustic backscatter from swath-mapping systems has the potential to provide near complete coverage of the bed (Brown and Blondel, 2009; Brown et al., 2011; Snellen et al., 2013), at resolutions down to a few centimeters, which photographic sampling could not practically achieve within the same time and with the same positional accuracy.

In shallow water, the physics of high frequency scattering of sound are relatively poorly understood, therefore acoustic sediment classification are almost always statistical (Snellen et al., 2013). Many such methods proposed to date are designed for characterizing large areas of seabed (Brown and Blondel, 2009; Brown et al., 2011) at relatively poor resolution (tens of meters to several hundred meters) and therefore rely on aggregation of data over scales much larger than the typical scales of sediment patchiness on heterogeneous riverbeds. In response to this need, Buscombe et al. (2014b, 2014c) developed a new statistical method for acoustic sediment classification based on spectral analysis of backscatter. This method is both continuous in coverage and of sufficient resolution (order meter or less) to characterize sediment variability on patchy riverbeds. Here, we apply these methods to multibeam echosounder (MBES) data collected from the bed of the Colorado River in Marble and Grand Canyons.

Sediment dynamics on the Colorado River in Grand Canyon National Park have been studied for several decades (e.g. Howard and Dolan, 1981; Rubin et al., 2002). Particular focus has been given to sandbars in large eddies downstream of tributary debris fans (Schmidt, 1990) because they are considered valuable resources by stakeholders and managers. Due to the severe limitations in sand supply imposed by Glen Canyon Dam (Howard and Dolan, 1981; Topping et

al., 2000; Hazel et al., 2006), understanding the effectiveness of sandbar management practices, such as controlled floods (Rubin et al. 2002; Topping et al., 2006; Hazel et al., 2010), and the long-term fate of sand in Grand Canyon over decadal timescales, requires construction of accurate sand budgets, which involves detailed monitoring of influx, efflux and changes in sand storage (Topping et al., 2000; Topping et al., 2010; Grams et al., 2013) and assessments of uncertainties in sand-budget calculations (Grams et al., 2013).

In order to estimate the sand budget, it is necessary to estimate what component of observed morphological changes is sand and what component is coarser. Grams et al. (2013) classified sand and coarse substrates using topographic roughness derived from digital elevation models, but the classification skill was estimated to be only 60-70%. In addition, sand bedforms had to be delineated manually, and validation was based on grain-size observations with positional uncertainties up to tens of meters. Because the morphology of the Colorado riverbed in Grand Canyon is mapped - to a large extent - using MBES (Kaplinski et al., 2009), the primary motivation for the present study is to examine how uncertainties in sand budgets can be constrained by producing maps of surface sediment types using the completely automated methods of Buscombe et al (2014b, 2014c) based on statistical analysis of MBES acoustic backscatter.

SITES AND DATA

MBES soundings, backscatter and underwater video camera images were collected in August 2013 from three short (approx. 500-1000m) reaches around sediment and flow gaging stations (Figure 1). Site 1 (hereafter, RM30), in Upper Marble Canyon at river-mile 30, is a relatively straight section of channel within the Redwall Limestone above Shinumo Wash. Site 2 (hereafter, RM61), in Lower Marble Canyon at river-mile 60, is within the Tapeats Sandstone just above the confluence with the Little Colorado River. Site 3 (hereafter, RM87), in Eastern Grand Canyon at river-mile 87, near Phantom Ranch within the Upper Granite Gorge, comprises two sections separated by a riffle and debris fan on river left. These sites were chosen to test scattering signatures of bed sediment because they collectively include a majority of the range of sediment, flow, geomorphic and geological settings found in this canyon river.

MBES data were collected using a Reson® 7125 multibeam sonar, operating at 400 kHz with a configuration that produces a 512 beam swath across a total subtended angle of 135°. This geometry permits swath widths of up to seven times the water depth. Each beam has a 0.5° across-track by 1.0° along-track angular width. Each echo is registered simultaneously by all 512 beams, which constitutes one ping. Pings are recorded up to 50 times per second. More details of sonar data collection are described in Kaplinski et al. (2009, 2014).

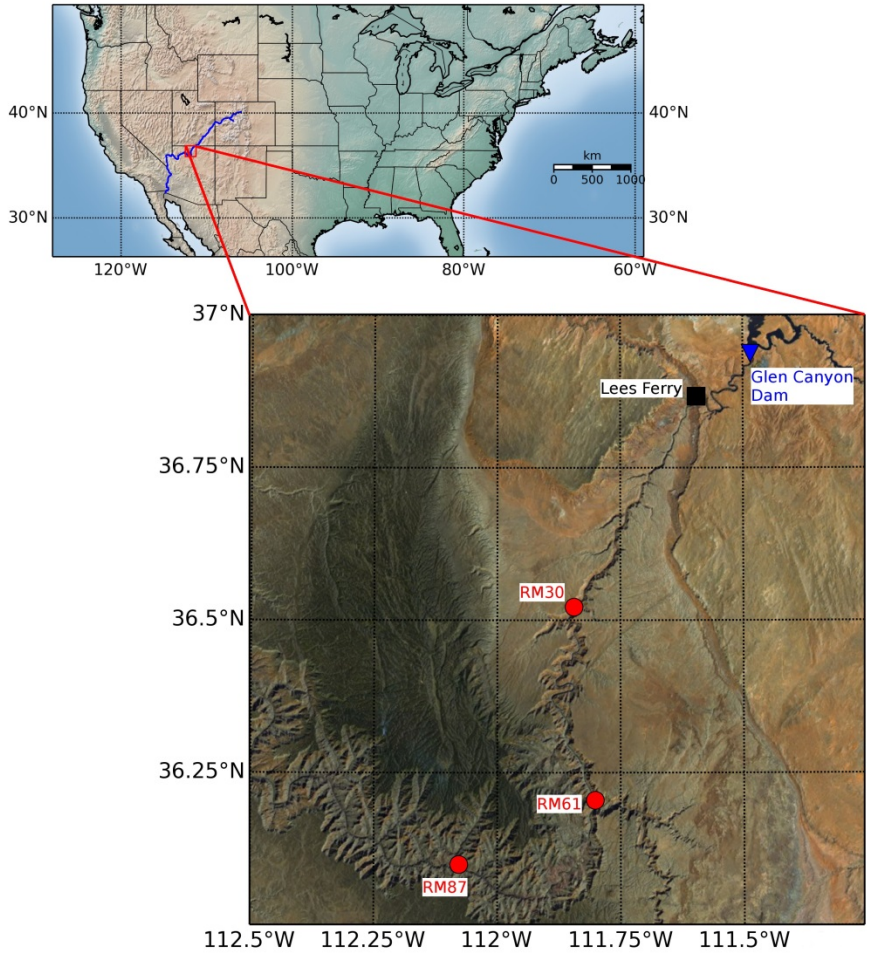

Figure 1 Map of survey locations on the Colorado River in Marble (RM30 and RM61) and Grand (RM87) Canyons.

A cabled video-microscope system was used to collected high-resolution (0.02mm/pixel) images of the bed. The system consists of a video camera fitted with macro lens, inside a protective metal housing. The transparent faceplate of the camera housing, fitted with LED lights for illumination, makes contact with the bed. Data collection involves navigating to each location, turning the boat to face the current, and lowering the video to the bed using an electric winch. The video is relayed instantly to the winch operator. For more details about the system, see Rubin et al. (2007, 2010). Coordinates of sample locations were measured by tracking the boat using a shore-based robotic laser-tracking system from established survey control points (Kaplinski et al., 2009). This method allows bed-sediment sampling at moderately high spatial density (up to tens of samples over tens of square meters) (Rubin et al., 2010) and hundreds of images can be obtained in a few hours. Another advantage of this approach over conventional physical sampling is that it samples only those sediments that are exposed on the bed surface. This is important because, given the high frequency of the MBES sound source, acoustic penetration into the bed is negligible, therefore the measured backscatter amplitude reflects the

composition of bed surface sediment (and possibly form roughness within the beam footprint) only.

The underwater video camera images were used to characterize bed-sediment, at a point, into three categories: 1) ‘sand’: homogeneous sandy surfaces (where no distinction was made between plane bed, ripples and dunes); 2) ‘gravel’: coarse substrates encompassing homogeneous gravels and sand-gravel mixtures (sand in the interstitial spaces of gravel clasts), in the size range deemed to be movable by typical flows; and 3) ‘rock’, a category which includes boulders, bedrock ledges, and cobbles large enough to be considered immovable by typical flows. These qualitative assessments were made by an experienced field technician operating the winch, based on both the image and the feel of the winch as the video housing hit the bed surface.

Figure 2 Underwater video images along a ~50m (river left to river right) transect at RM 30, showing typical sediment heterogeneity.

Another underwater video camera system - a towed video sled with a wider field of view, equipped with powerful lights and lasers for scale - was also used to observe the bed. These data were collected at a different time (May 2012) in the RM30 and RM61 pools, along with MBES data, and were used to assess the plausibility of sediment classifications applied to an earlier data set (outside the calibration).

DATA PRE-PROCESSING

Several quality control and quality assurance procedures are performed to ensure only high-quality amplitude data are used for bed sediment characterization. These checks, detailed in Kaplinski et al. (2009, 2014) and Buscombe et al. (2014b), include:

1. Patch tests to determine the offset angles and timing between the various system components.
2. Beam-angle tests are used to determine the uncertainty of soundings for all beam angles.
3. Quality assurance assessments performed in real time during the surveys by continuously monitoring across-track swaths and comparison between adjacent overlapping sweeps.
4. Manual sweep editing and systematically stepping through overlapping sweeps.
5. Automated spatial filtering procedures, designed to identify artifacts based on excessive bathymetric slopes; and incorrect beam locations.

The raw high-frequency echoes recorded by the receive beams MBES are corrected for beam geometry effects (angle of sound incidence and area of beam of the sloping bed) and radiometric effects (source and transmission losses) using the methods detailed in Buscombe et al. (2014b). Backscatter was corrected for water and suspended sediment attenuation using the median size and concentration of sand, and concentration of silt and clay. These were available every 15 minutes from gages in the same survey reach (Griffiths et al., 2012). It was assumed that the median silt grain size is 2 μm (Voichick and Topping, 2014). It was further assumed that sand and silt are homogeneously mixed through the water column. This assumption is physically unreasonable for sand. However, sand suspensions were so dilute so as to make negligible difference to the sediment attenuation calculation, so the assumption of homogeneous mixing was made for numerical convenience. For water attenuation corrections, measurements of temperature and salinity were also available every 15 minutes from sondes at each gaging station.

SPECTRAL ANALYSIS

Backscatter data from the three survey reaches were processed using the spectral analysis methods presented in Buscombe et al. (2014b) which use the (per beam, per ping) amplitudes of backscattered sound associated with time-of flight bathymetric soundings (range to the bed). This recorded amplitude is either the peak amplitude, or the amplitude associated with the highest phase-coherence between the source sound wave envelope and the echo wave envelope. Either way, it is considered the integral of the portion of reflected sound at incidence angle from all scatterers in the insonified area of the bed (the beam footprint).

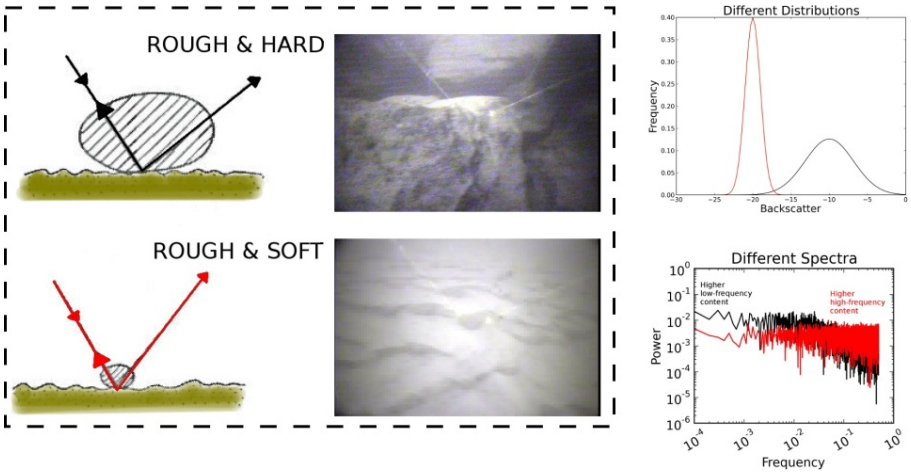

Figure 3 Schematic showing hypothesized backscatter distributions and spectra for rough/hard substrate (rock) and rough/soft substrate (rippled sand).

The method quantifies the variation in length- and amplitude-scales of backscatter over small areas of gridded surfaces, using windowed spectral (frequency domain) analysis (Figure 3). Because backscatter is a measure of the hardness (impedance) of a substrate, this approach is somewhat independent of the roughness of the topography, which may not be uniquely related to

a given substrate type (for example, the occurrence of gravel dunes). The method works by carrying out spectral analysis of gridded backscatter (the median value per grid cell) that has been detrended and tapered (Figure 4). Backscatter power spectra are computed to produce scale and amplitude metrics that collectively characterize the length scales of stochastic measures of riverbed scattering, termed `stochastic geometries' by Buscombe et al. (2014b). Backscatter aggregated over small spatial scales has spectra that obey a power-law in 1D (Figure 4). Relationships exist between stochastic geometries of backscatter and areas of rough and smooth sediments (Buscombe et al., 2014c).

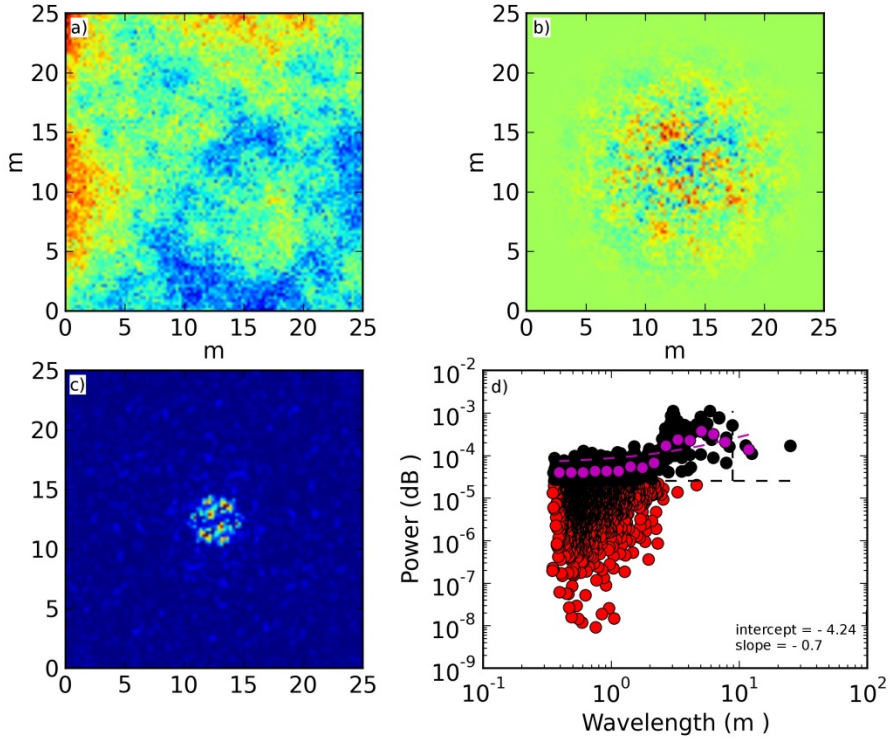

Figure 4 A window of backscatter (a) is detrended and Hann tapered (b). The 2D power spectral density of this surface (c) is collapsed to a 1D form (d) from which statistics are calculated (from the data that are statistically significant at the 95% level, shown as black dots) such as the slope and the intercept. These statistics have been shown to be sensitive to changing substrate type by Buscombe et al. (2014b, 2014c).

A grid size of 0.25 x 0.25 m was chosen for construction of surfaces because this was the smallest scale at which there were, consistently across sites, multiple usable soundings. A window size of 25 x 25 m was chosen based on examination of individual spectra and the criteria suggested by Buscombe et al (2014c). Windows are moved around the surface such that the outputs from one window are ascribed to the central cell of the window. The window is then shifted by a specified amount in space in 2 directions, and the calculations are repeated. This process is repeated until the entire surface has been analyzed by systematic windowing. A shift length of 0.25 m (1 grid cell) was chosen so the output surfaces were the same spatial resolution

as the input surfaces. In this configuration, the value in each output grid cell is the ensemble average of 1000 individual spectra for a window passing over that point.

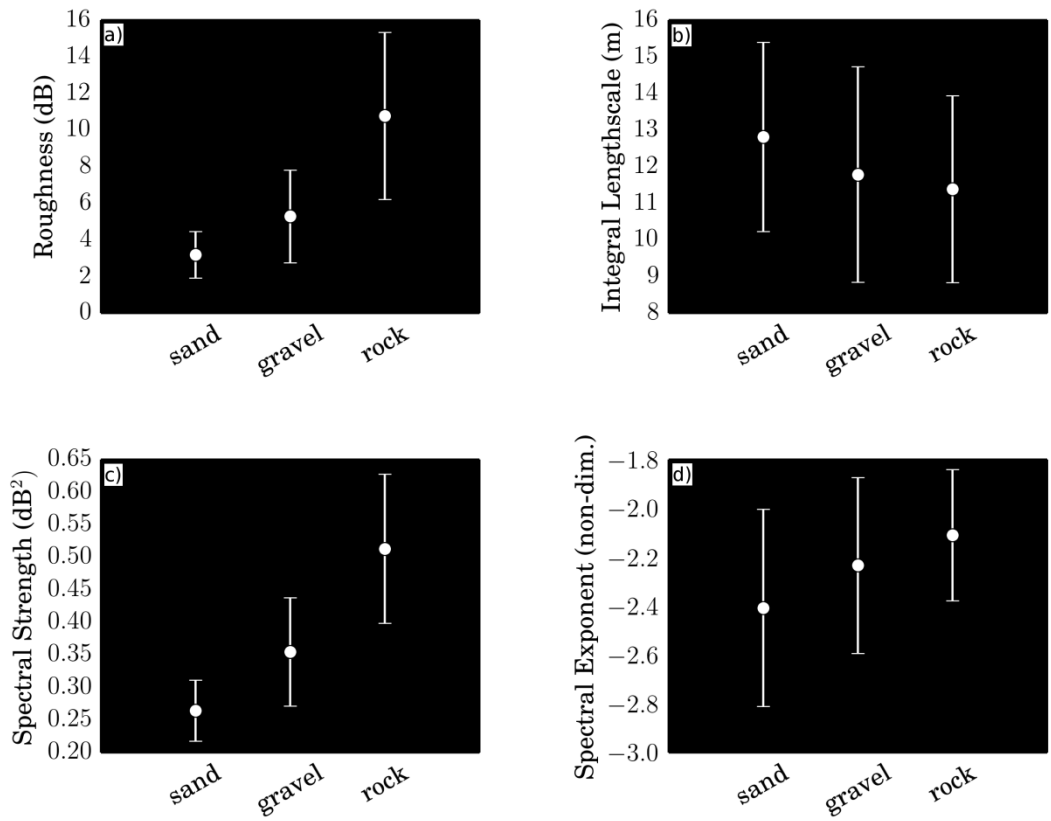

Figure 5 Example of spectral signatures of 3 different sediment substrates at RM 87. Roughness (a) is the root mean square variance in amplitude; integral lengthscale (b) is a measure of persistence; spectral strength (c) is a measure of power at low frequencies; and spectral exponent (d) is a measure of the rate of decay of power with increasing frequency. In each subplot, the dot represents the mean quantity per co-located substrate and the bars are the range of values.

SEDIMENT SPECTRAL SIGNATURES

Four parameters are calculated from each computed log-transformed spectrum, according to the methods detailed in Buscombe et al (2014b): 1) the spectral strength, ω, which is the intercept of the regression through the statistically significant portion of the spectrum, and a measure of the variance in the data at low frequencies (large wavelengths); 2) the spectral exponent, γ, which is the slope of the regression through the statistically significant portion of the spectrum, and a measure of the decay in power as a function of frequency, or the number of frequencies required to describe the data (spectral width) and therefore a measure of how complicated the data is; 3) the acoustic 'roughness', σ, which is the overall power in the spectrum over all frequencies; and 4) the integral lengthscale, which describes the lengthscale over which the surface is typically statistically significant. These 4 parameters were found by Buscombe et al (2014c) to have the

strongest correlations with co-located substrate types (Figure 5) identified in the underwater video streams. Of these, the spectral strength, exponent and roughness were used to develop an acoustic sediment classification because they have high between-substrate variability, low between-site variability, low within-substrate variability, and the magnitude of values scale with substrate size.

SEDIMENT CLASSIFICATION

Towards an aim of classifying each 0.25 × 0.25 m grid cell into three sediment types, Buscombe et al. (2014c) developed an approach based on decision tree learning. A decision tree (Breiman et al., 1984) recursively partitions the space into smaller homogeneous subsets using a set of binary condition rules such that the samples with the same labels are grouped together. The basic process is as follows: 1) for each attribute (spectral slope, strength, and roughness), find the feature that best divides the training data (attribute value at each substrate location) such as information gain from splitting on the attribute; 2) create a decision node that splits on the attribute with the highest information gain; and 3) recurse over the sub-lists obtained (at descendant nodes) by splitting on the previous decision node until no more splits are possible. More details are provided in Buscombe et al. (2014c).

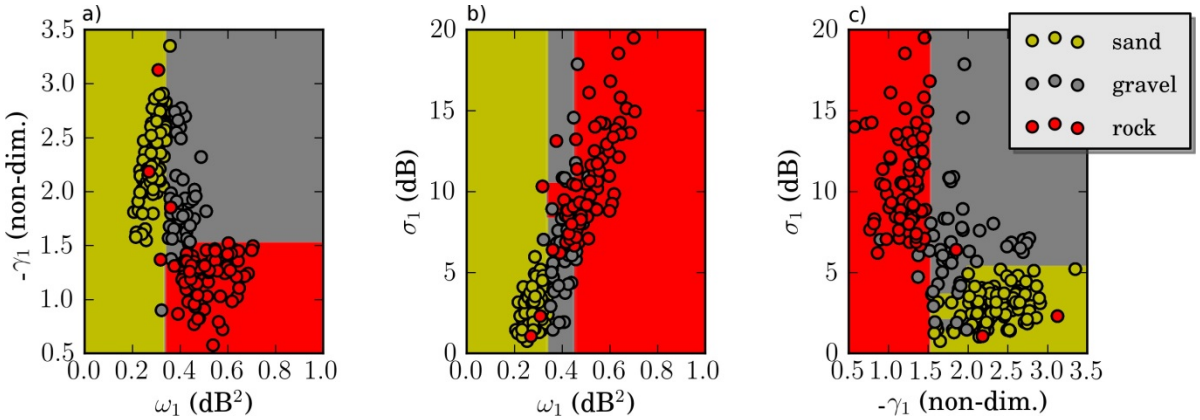

Figure 6 Decision surfaces of paired parameters based on aggregation of observations from RM30, RM60 and RM87 pools (circles), with a constraint that each decision node must have at least 50 samples: (a) ω and -γ ; (b) ω and σ; and (c) -γ and σ. The yellow, grey and red portions of the parameter space show where the decision tree would classify as sand, gravel and rock, respectively.

Classifications were carried out using a calibration based on data aggregated from all three sites (RM 30, RM 61, and RM 87). Trees were constructed with a single constraint that a minimum of 50 samples were required to be at a terminal node. The decision surface (Figure 6) shows the observations as colored markers, and a relatively straightforward partitioning of space between pairs of the 3 spectral parameters input into the decision tree algorithm. An example work flow from map of gridded corrected backscatter, to maps of spectral quantities with the same resolution, to final classification, has been provided for the RM 30 site (Figure 7). The classification skill for sand, gravel and rock is 97, 81, and 95 % respectively. Finally, another

sediment classification map is provided for RM 61 (Figure 8) overlying an aerial photo for geomorphic context.

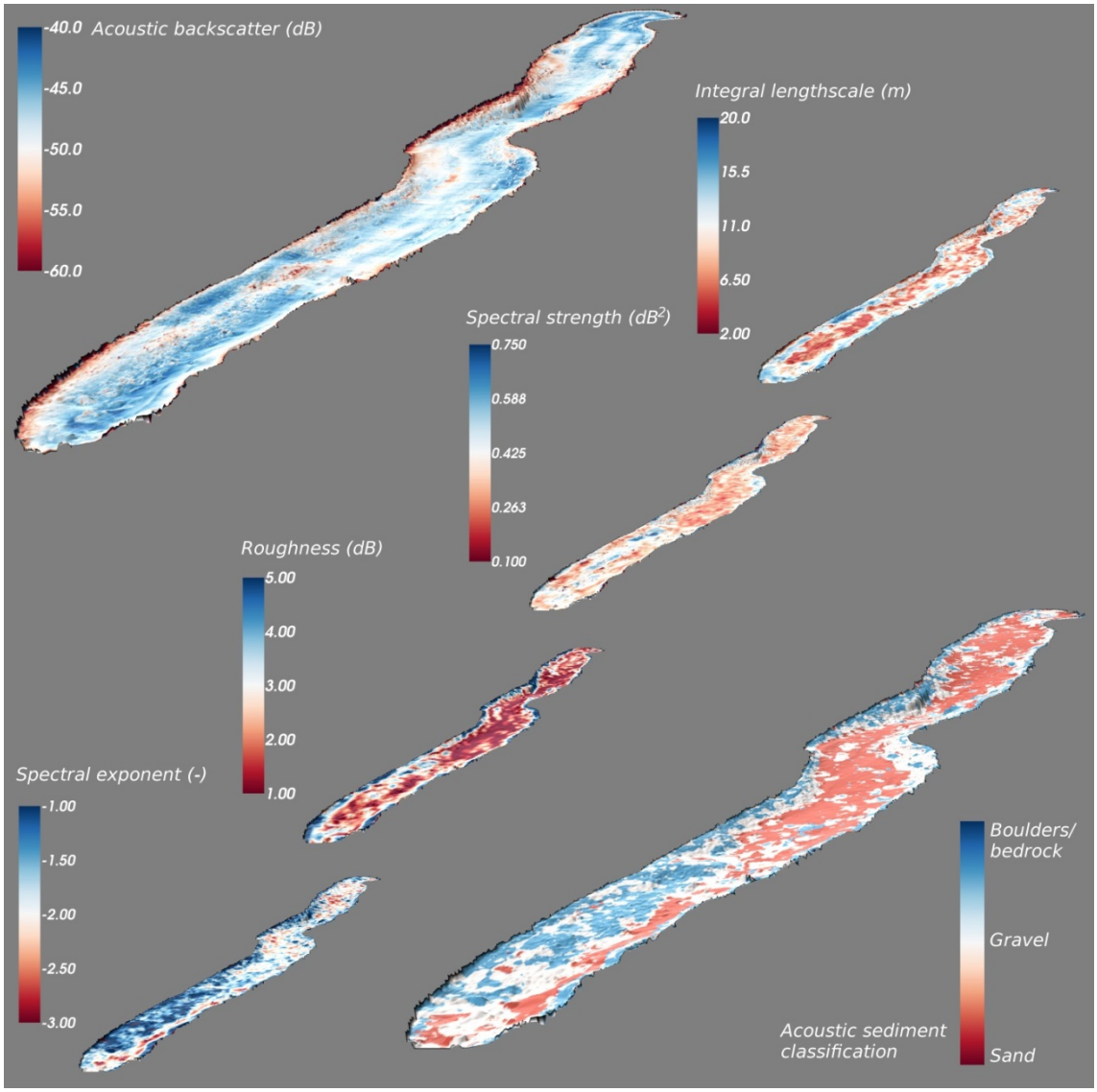

Figure 7 Example of processing stages from data collected at RM 30. Upstream to downstream is bottom left to upper right. Each map is a 3D DEM of the survey pool draped with a different quantity. From gridded acoustic backscatter (top), various maps of spatially explicit stochastic geometries (middle), derived from the windowed spectral analysis procedure, are merged in a decision tree classification to produce a map of sediment types (bottom).

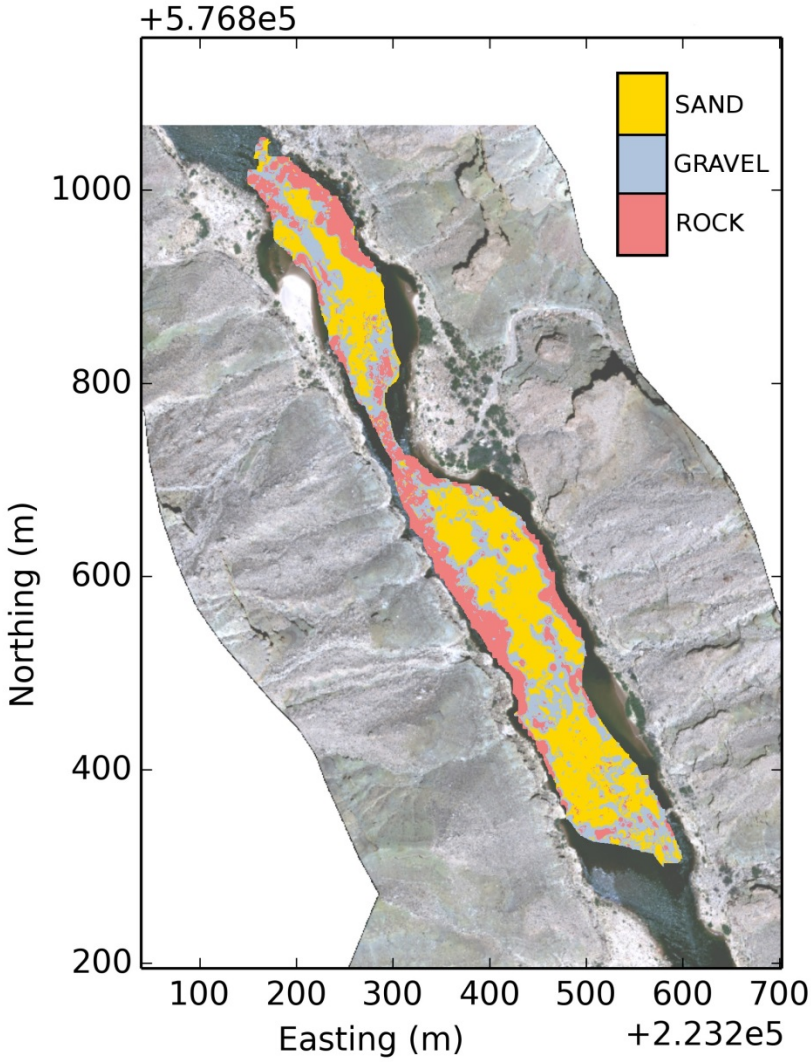

Figure 8 Example of sediment classification map at RM 61.

SUMMARY

Capturing the spatial variability in classifications of riverbed sediments is challenging using high-frequency hydro-acoustic instruments. However, the method proposed by Buscombe et al (2014b, 2014c) has been shown to be potentially useful to classify grain-scale roughness and hardness on the Colorado riverbed in Marble and Grand Canyons. The method uses high-frequency acoustic backscatter from multibeam sonar to classify heterogeneous riverbed sediments by type (sand, gravel, rock) continuously in space and at small spatial resolution.

Spatially explicit maps of the stochastic geometries (length- and amplitude-scales) of backscatter are related to patches of riverbed surfaces composed of known sediment types, as determined by geo-referenced underwater video observations. Statistics of backscatter magnitudes alone are found to be poor discriminators between sediment types. However, the variance of the power spectrum, and the intercept and slope from a power-law spectral form (termed the spectral

strength and exponent, respectively) successfully discriminate between sediment types. A decision tree approach to classifications was able to classify spatially heterogeneous patches of homogeneous sands, gravels (and sand-gravel mixtures), and cobbles/boulders with 95, 88, and 91% accuracy, respectively. This data-driven approach allows bed sediment classifications at unprecedented resolution.

REFERENCES

Brown, C.J., and Blondel, P. (2009). "Developments in the application of multibeam sonar backscatter for seafloor habitat mapping," Applied Acoustics (70), pp. 1242-1247.

Brown, C.J., Smith, S.J., Lawton, P., and Anderson, J.T. (2011). "Benthic habitat mapping: A review of progress towards improved understanding of the spatial ecology of the seafloor using acoustic techniques," Estuarine, Coastal and Shelf Science (92), pp. 502-520.

Breiman, L., Friedman, J.H., Olshen, R.A., Stone, C.J. (1984). Classification and regression trees. Wadsworth and Brooks/Cole Advanced Books and Software, Monterey, California.

Buscombe, D., Rubin, D.M., Lacy, J.R., Storlazzi, C.D., Hatcher, G., Chezar, H., Wyland, R., and Sherwood, C.R. (2014a). "Autonomous bed-sediment imaging-systems for revealing temporal variability of grain size," Limnology and Oceanography: Methods (12), pp. 390-406.

Buscombe, D., Grams, P.E., and Kaplinski, M.A. (2014b). "Characterizing riverbed sediments using high-frequency acoustics 1: Spectral properties of scattering," Journal of Geophysical Research - Earth Surface (119), F003189, doi:10.1002/2014JF003189.

Buscombe, D., Grams, P.E., and Kaplinski, M.A. (2014c). "Characterizing riverbed sediments using high-frequency acoustics 2: Scattering signatures of Colorado River bed sediments in Marble and Grand Canyons," Journal of Geophysical Research - Earth Surface (119), JF003191, doi:10.1002/2014JF003191.

Dietrich, W.E., and Smith, J.D. (1984). "Bed load transport in a river meander," Water Resources Research (20), pp. 1355-1380.

Grams, P.E., Topping, D.J., Schmidt, J.C., Hazel, J.E., and Kaplinski, M.A. (2013). "Linking morphodynamic response with sediment mass balance on the Colorado River in Marble Canyon: Issues of scale, geomorphic setting, and sampling design," Journal of Geophysical Research - Earth Surface (118), pp. 361-381.

Griffiths, R.E., Topping, D.J., Andrews, T., Bennett, G.E., Sabol, T.A., and Melis, T.S. (2012). "Design and maintenance of a network for collecting high-resolution suspended-sediment data at remote locations on rivers, with examples from the Colorado River." U.S. Geological Survey Techniques and Methods, book 8, chapter C2, 44 p.

Hazel, J.E., Grams, P.E., Schmidt, J.C., Kaplinski, M. (2010). "Sandbar response following the 2008 high-flow experiment on the Colorado River in Marble and Grand Canyons," U.S. Geological Survey Scientific Investigations Report 2010-5015, 52 pp.

Hazel, J.E., Topping, D.J., Schmidt, J.C., and Kaplinski, M.A. (2006). "Influence of a dam on fine-sediment storage in a canyon river," Journal of Geophysical Research - Earth Surface (111), pp. F01025.

Howard, A., and Dolan, R. (1981). "Geomorphology of the Colorado River in the Grand Canyon," The Journal of Geology (89), pp. 269-298.

Kaplinski, M.A., Hazel, J.E., Grams, P.E., and Davis, P.A. (2014). "Monitoring fine-sediment volume in the Colorado River ecosystem, Arizona: Construction and analysis of digital elevation models," U.S. Geological Survey Open-File Report 2014-1052, 29 pp.

Kaplinski, M.A., Hazel, J.E., Parnell, R., Breedlove, M., Kohl, K., and Gonzales, M. (2009). "Monitoring fine-sediment volume in the Colorado River Ecosystem, Arizona: Bathymetric survey techniques," U.S. Geological Survey Open-File Report 2009-1207, 41 pp.

Nelson, P.A., Bellugi, D., and Dietrich, W.E. (2014). "Delineation of river bed-surface patches by clustering high-resolution spatial grain size data," Geomorphology (205), pp. 102-119.

Rubin, D.M., Chezar, H., Harney, J.N., Topping, D.J., Melis, T.S., and Sherwood, C.R. (2007). "Underwater microscope for measuring spatial and temporal changes in bed-sediment grain size," Sedimentary Geology (202), pp. 402-408.

Rubin, D.M., Topping, D.J., Chezar, H., Hazel, J.E., Schmidt, J.C., Breedlove, M., Melis, T.S., Grams., P.E. (2010). "20,000 grain-size observations from the bed of the Colorado River, and implications for sediment transport through Grand Canyon," 9th Federal Interagency Sedimentation Conference.

Rubin, D.M., Topping, D.J., Schmidt, J.C., Hazel, J.E., Kaplinski, M., and Melis, T.S. (2002). "Recent sediment studies refute Glen Canyon Dam hypothesis," Eos (Transactions, American Geophysical Union) (83), pp. 277-278.

Schmidt, J.C. (1990). "Recirculating flow and sedimentation in the Colorado River in Grand Canyon, Arizona," The Journal of Geology (98), pp. 709-724.

Snellen, M., Eleftherakis, D., Amiri-Simkooei, A., Koomans, R.L., and Simons, D.G. (2013). "An inter-comparison of sediment classification methods based on multi-beam echo-sounder backscatter and sediment natural radioactivity data," Journal of the Acoustical Society of America (134), 959-970.

Topping, D.J., Rubin, D.M., Grams, P.E., Grifths, R.E., Sabol, T.A., Voichick, N., Tusso, R.B., Vanaman, K.M., and McDonald, R.R. (2010). "Sediment transport during three controlled-flood experiments on the Colorado River downstream from Glen Canyon Dam, with implications for eddy-sandbar deposition in Grand Canyon National Park," U.S. Geological Survey Open-File Report 2010-1128, 111 pp.

Topping, D.J., Rubin, D.M., Schmidt, J.C., Hazel, J.E., Melis, T.S., Wright, S.A., Kaplinski, M., Draut, A.E., and Breedlove, M.J. (2006). "Comparison of sediment-transport and bar-response results from the 1996 and 2004 controlled-flood experiments on the Colorado River in Grand Canyon," 9th Federal Interagency Sedimentation Conference.

Topping, D.J., Rubin, D.M., and Vierra, L.E.J. (2000). "Colorado River sediment transport 1. Natural sediment supply limitation and the influence of Glen Canyon Dam," Water Resources Research (36), pp. 515-542.

Voichick, N., and Topping, D.J. (2014). "Extending the turbidity record – making additional use of continuous data from turbidity, acoustic-Doppler, and laser diffraction instruments and suspended-sediment samples in the Colorado River in Grand Canyon," U.S. Geological Survey Scientific Investigations Report 2014-5097, 31 p.

®, Any use of trade, product, or names is for descriptive purposes only and does not imply endorsement by the U.S. government.